Spontaneous Formation of Vesicles and Chiral Self-Assemblies of Sodium *N*-(4-Dodecyloxybenzoyl)-L-valinate in Water

Ashok Mohanty and Joykrishna Dey*

Department of Chemistry, Indian Institute of Technology, Kharagpur-721 302, India

Received October 21, 2003. In Final Form: May 21, 2004

A novel *N*-acylamino acid surfactant, sodium *N*-(4-dodecyloxybenzoyl)-L-valinate (SDLV), has been synthesized. The aggregation behavior of the surfactant in aqueous solution has been studied by surface tension, fluorescence probe, microscopy, and dynamic light scattering (DLS) techniques. The amphiphile has a very low critical aggregation concentration (cac). These studies have suggested formation of large bilayer structures in water. The mean apparent hydrodynamic radius, R_H, of the self-assemblies in dilute aqueous solution obtained from DLS measurements confirmed formation of large aggregates. The FT-IR spectra of the amphiphile have indicated strong intermolecular amide hydrogen bonding in the self-assemblies in aqueous solution. The microenvironment of the fluorescence probes is highly nonpolar and viscous in nature. The circular dichroism (CD) spectra of SDLV were recorded in water and in a 1:1 water−methanol mixture. The CD spectra have indicated the presence of chiral aggregates in aqueous solution above the cac. The microstructure of the aggregates has been studied by use of optical and transmission electron microscopy. Both types of micrographs have shown the presence of a variety of morphologies including giant spherical vesicles, tubules, twisted ribbons, and helical strands in aqueous solutions.

Introduction

Like the formation of micelles, the formation of vesicles is a result of the energetically favorable hydrophobic association of the hydrocarbon tail(s) of an amphiphilic molecule. The vesicles have two distinct domains: the lipophilic membrane and the interior aqueous cavity. The syntheses of amphiphilic molecules with different structures that can self-organize to form vesicles have been reported by many authors.[1] This is because of their importance in chemistry and biology as well as in industry.[2,3] There is a considerable body of literature that addresses vesicles and liposomes used in various scientific fields.[4] Vesicles are increasingly being used in commercial products. Since vesicles can entrap large quantities of reagents either in the lipophilic membrane or in the aqueous cavity, they have been used as encapsulants of cosmetic substances and pharmaceutical drugs. Liposomes have potential use as controlled drug delivery vehicles in the pharmaceutical industry. Also, vesicles have some important characteristics that allow them to be used as sensitive reagents for analytical detection.[5] Lundhal and Yang have used liposomes for separating biomolecules.[6] Recently, the separation of other types of molecules has also been suggested in the literature.[7] In fact, the present authors have reported the use of giant vesicles as a pseudostationary phase in the enantiomeric separation of (±)-binaphthol and (±)-binaphthol phosphate by use of the micellar electrokinetic capillary chromatographic technique.[8]

Normally vesicles are formed by amphiphiles containing double hydrocarbon chains. However, recently many authors have reported formation of vesicular structures by single-chain amphiphiles.[1h,i,9] Single-chain amphiphiles that form vesicular structures usually have unsaturation, have a biphenyl or diphenylazomethine group, or have hydrogen-bond-forming groups in the hydrocarbon chain. Vesicles have also been produced in solution by mixing two or more single-chain surfactants or cosurfactants.[10] The catanionic (or ion-pair) surfactants fall in this class. More recently, many amphiphiles have been reported to

* To whom correspondence should be addressed. Telephone: 91-3222-283308. Fax: 91-3222-255303. E-mail: joydey@chem.iitkgp.ernet.in.

(1) (a) Martinez, J. S.; Zhang, G.; Holt, P.; Jung, H.-T.; Carrano, C. J.; Haygood, M. G.; Butler, A. *Science* **2000**, *287*, 1245. (b) Putlitz, B. Z.; Hentz, H. P.; Landfester, K.; Antonietti, M. *Langmuir* **2000**, *16*, 3003−3005. (c) Bandopadhyay, P.; Bharadwaj, P. K. *Langmuir* **1998**, *14*, 7537. (d) Kimizuka, N.; Wakiyama, T.; Miyauchi, H.; Yoshimi, T.; Tokuhiro, M.; Kunitake, T. *J. Am. Chem. Soc.* **1996**, *118*, 5808. (e) Schenning, A. P. H.; Bruin, B. De; Feiters, M. C.; Nolte, R. J. M. *Angew. Chem., Int. Ed. Engl.* **1994**, *33*, 1662. (f) Waggoner, T. A.; Last, J. A.; Kotula, P. G.; Sasaki, D. Y. *J. Am. Chem. Soc.* **2001**, *123*, 496. (g) Constable, E. C.; Meier, W.; Nardin, C.; Mundwiler, S. *J. Chem. Soc., Chem. Commun.* **1999**, 1483. (h) Kunitake, T.; Okahata, Y.; Shimomura, M.; Yasunami, S.; Takarabe, K. *J. Am. Chem. Soc.* **1993**, *115*, 3840. (i) Kunitake, T. *Angew. Chem., Int. Ed. Engl.* **1992**, *31*, 709.

(2) Sumida, Y.; Masuyama, A.; Takasu, M.; Kida, T.; Nakatsuji, Y.; Ikeda, I.; Nojima, M. *Langmuir* **2001**, *17*, 609.

(3) (a) *Handbook of Nonmedical Applications of Liposomes*: Lasic, D. D., Barenholz, Y., Eds.; CRC Press: New York, 1996; Vol. 4. (b) Lasic, D. D. In *Vesicles*; Rosoff, M., Ed.; Marcel Dekker: New York, 1996; Vol. 62, pp 447−476. (c) Lasic, D. D. *Liposomes in Gene Delivery*; CRC Press: New York, 1997. (d) *Gene Therapy Technologies, Applications, and Regulations*; Meager, A., Ed.; John Wiley & Sons: New York, 1999. (e) Needham, D.; Lasic, D. D. *Chem. Rev.* **1995**, *95*, 2601.

(4) Frendler, J. *Membrane Mimetic Chemistry*; Wiley: New York, 1983.

(5) (a) Plant, A. L.; Brizgys, M. V.; Locasio, L. E.; Durst, R. A. *Anal. Biochem.* **1989**, *176*, 420−426. (b) Locascio-Brown, L.; Plant, A. L.; Horvath, V.; Durst, R. A. *Anal. Chem.* **1990**, *62*, 2587−2593. (c) Reeves, S. G.; Rule, G. S.; Roberts, M. A.; Edwards, A. J.; Durst, R. A. *Talanta* **1994**, *41*, 1747−1753.

(6) Lundhal, P.; Yang, Q. *J. Chromatogr.* **1991**, *544*, 283−304.

(7) Hong, M.; Weekley, B. S.; Grieb, S. J.; Foley, J. P. *Anal. Chem.* **1998**, *70*, 1394−1403 and references therein.

(8) Mohanty, A.; Dey, J. *J. Chem. Soc., Chem. Commun.* **2003**, 1384−1385.

(9) (a) Dey, J.; Roy, S. *Langmuir* **2003**, *19*, 9625. (d) Tachibana, T.; Yoshizumi, T.; Hori, K. *Bull. Chem. Soc. Jpn.* **1979**, *52*, 34−41 and references therein.

(10) (a) Kaler, E. W.; Murthy, A. K.; Rodriguez, B.; Zasadzinski, J. A. *Science* **1989**, *245*, 1371. (b) Kaler, E. W.; Herrington, K. L.; Murthy, A. K.; Zasadzinski, J. A. *J. Phys. Chem.* **1992**, *96*, 6698. (c) Herrington, K. L.; Kaler, E. W.; Miller, D. D.; Zasadzinski, J. A.; Chirulvolu, S. *J. Phys. Chem.* **1993**, *97*, 13792. (d) Marques, E. *Langmuir* **2000**, *16*, 156.

10.1021/la035958x CCC: $27.50
Published on Web 08/26/2004

form vesicular structures in dilute aqueous solutions induced by metal ions.[1a,11] Single-chain chiral amphiphiles are also known to form a variety of aggregates including vesicles.[12−15] Since chiral surfactants have been shown to be useful in stereoselective synthesis[16] and in enantiomeric separation of pharmaceuticals,[17] the study of surfactants with chiral centers has become more popular. It has been shown that the nature of vesicular structures used for controlled drug delivery depends on the stereochemistry of the chiral amphiphile.[18] The chiral centers in biological lipids often control the nature of their self-assemblies under physiological conditions.[19] Therefore, there is a great demand for a thorough understanding of the effect of molecular stereochemistry in surfactant self-assembly in the field of biomedical research. Consequently, the *N*-acylamino acid surfactants (NAASs) have attracted considerable attention in recent years.[13−15] The NAASs show some characteristic chirality-dependent properties in solution. For example, an optically active NAAS always has a lower critical micelle concentration than its racemic isomer.[20] Also, an optically active NAAS forms lyotropic liquid crystals different from its racemic isomer.[21] The optically active NAASs have been shown to form chiral aggregates through intermolecular amide−amide hydrogen bonding.[15] Indeed, these amphiphiles form aggregates, which have a variety of morphologies including vesicles, tubules, ribbons, and helical structures. In a recent communication, we have shown by optical microscopic studies that sodium *N*-(4-dodecyloxybenzoyl)-L-valinate, SDLV (see Figure 1 for molecular structure), spontaneously forms giant vesicles in dilute aqueous solutions.[8] We have demonstrated that self-assemblies of SDLV act as a very good chiral selector for the enantioseparation of (±)-binaphthol and (±)-binaphthol phosphate by use of the micellar electrokinetic capillary chromatographic technique.[8]

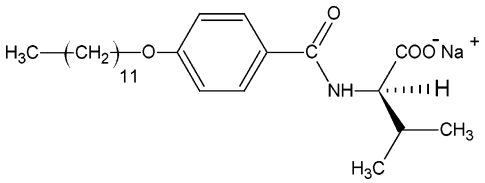

Figure 1. Molecular structure of SDLV.

To understand the improved chiral selectivity of SDLV compared to those reported in the literature, we have undertaken this work to study its aggregation behavior in aqueous solution. In the present work, we have investigated in detail the self-organization properties of SDLV in aqueous solutions by use of various techniques such as surface tension, fluorescence, dynamic light scattering (DLS), circular dichroism (CD), and microscopy. The focus of this work is (i) to investigate the surface and aggregation properties of SDLV in aqueous solutions, (ii) to study the microenvironment of the self-assemblies in water, (iii) to determine the mean size of the aggregates formed, (iv) to examine the CD spectra for chiral self-assemblies of SDLV, and (v) to investigate the solution microstructure of the self-assemblies. The role of intermolecular secondary amide hydrogen bonds in the formation of bilayer structures in aqueous solutions has also been discussed.

Results and Discussion

Surface Tension Measurements. The critical aggregation concentration (cac) of SDLV in water (pH 7.5) and 0.01 M NaOH solution (pH 11.5) was determined from the break point of the plot of surface tension γ versus log C (Figure 2). No minimum around the cac can be observed, confirming the purity of the surfactant. The cac values and the surface properties of the amphiphile are listed in Table 1. The cac value in NaOH solution is slightly greater than in water. The cac value and the surface tension at the cac are low, implying that SDLV is a very good surfactant. The low cac of SDLV is due to the long hydrophobic chain, which enhances the hydrophobic interaction. We believe that the $\pi-\pi$ interaction due to the phenyl ring also contributes to enhanced hydrophobic interactions. The low cac value in water might be due to the presence of the undissociated acid form of the amphiphile, which reduces headgroup repulsion and thus

(11) (a) Luo, X.; Wu, X.; Liang, Y. *J. Chem. Soc., Chem. Commun.* **2002**, 492. (b) Luo, X.; Miao, W.; Wu, S.; Liang, Y. *Langmuir* **2002**, *18*, 9611−9612.

(12) (a) Pfannemüller, B.; Kühn, I. *Makromol. Chem.* **1988**, *189*, 2433. (b) Emmanouil, V.; El Ghoul, M.; Andre-barres, C.; Guidette, B.; Rico-Lattes, I.; Lattes, A. *Langmuir* **1998**, *14*, 5389. (c) Fuhrop, J. H.; Blumtritt, P.; Lehmann, C.; Luger, P. *J. Am. Chem. Soc.* **1991**, *113*, 7437. (d) Nakashima, N.; Asakuma, S.; Kunitake, T. *J. Am. Chem. Soc.* **1985**, *107*, 509. (e) Frankel, D. A.; O'Brien, D. F. *J. Am. Chem. Soc.* **1991**, *113*, 7436. (f) Köning, J.; Boettcher, C.; Winkler, H.; Zeitler, E.; Talmon, Y.; Fuhrop, J. H. *J. Am. Chem. Soc.* **1997**, *115*, 693.

(13) (a) Du, X.; Hlady, V. *J. Phys. Chem. B* **2002**, *106*, 7295−7299. (b) Du, X.; Liang, Y. *J. Phys. Chem. B* **2001**, *105*, 6092. (c) Du, X.; Liang, Y. *J. Phys. Chem. B* **2000**, *104*, 10047. (d) Miyagishi, S.; Takeuchi, N.; Asakawa, T.; Inoh, M. *Colloids Surf., A* **2002**, *197*, 125−132. (e) Bella, J.; Borocci, S.; Mancini, G. *Langmuir* **1999**, *15*, 8025−8031. (f) Borocci, S.; Mancini, G.; Cerichelli, G.; Luchetti, L. *Langmuir* **1999**, *15*, 2627−2630. (g) Hoffmann, F.; Huhnerfuss, H.; Stine, K. *Langmuir* **1998**, *14*, 4525. (h) Parazak, D. P.; Uang, J. Y.-J.; Turner, B.; Stine, K. *Langmuir* **1994**, *10*, 3787.

(14) (a) Zhang, Y.-J.; Jin, M.; Lu, R.; Song, Y.; Jiang, L.; Zhao, Y. *J. Phys. Chem. B* **2002**, *106*, 1960−1967. (b) Boettcher, C.; Schade, B.; Fuhrhop, J.-H. *Langmuir* **2001**, *17*, 873−877. (c) Imae, T.; Takahashi, Y.; Muramatsu, H. *J. Am. Chem. Soc.* **1992**, *114*, 3414−3419. (d) Vollhardt, D.; Gehlert, U. *J. Phys. Chem. B* **2002**, *106*, 4419−4423. (e) Kawasaki, H.; Souda, M.; Tanaka, S.; Nemoto, N.; Karlsson, G.; Almgren, M.; Maeda, H. *J. Phys. Chem. B* **2002**, *106*, 1524−1527. (f) Fuhrop, J.-H.; Demoulin, C.; Rosenberg, J.; Boettcher, C. *J. Am. Chem. Soc.* **1990**, *112*, 2827−2829. (g) Fuhrop, J.-H.; Schnieder, P.; Rosenberg, J.; Boekema, E. *J. Am. Chem. Soc.* **1989**, *111*, 3387−3390.

(15) (a) Shinitzky, M.; Haimovitz, R. *J. Am. Chem. Soc.* **1993**, *115*, 12545−12549. (b) Song, J.; Cheng, Q.; Kopta, S.; Stevens, R. *J. Am. Chem. Soc.* **2001**, *123*, 3205. (c) Bhattacharyya, S.; Krishnan-Ghosh, Y. *J. Chem. Soc., Chem. Commun.* **2001**, 185. (d) Luo, X.; Liu, B.; Liang, Y. *J. Chem. Soc., Chem. Commun.* **2001**, 1556.

(16) (a) Zhang, Y.; Sun, P. *Tetrahedron*: *Asymmetry* **1996**, *7*, 3055. (b) Takeshita, M.; Yanagihara, H.; Terada, K.; Akutsu, N. *Annu. Rep. Tohoku Coll. Pharm.* **1992**, *39*, 247. (c) Zhan, Y.; Wu, W. *Tetrahedron*: *Asymmetry* **1999**, *8*, 3575−3578. (d) Diego-Castro, M. J.; Hailes, H. C. *Chem. Commun.* **1998**, 1549−1550.

(17) (a) Clothier, J.; Tomellini, S. *J. Chromatogr., A* **1996**, *723*, 179. (b) Desbene, P.; Fluchic, C. *J. Chromatogr., A* **1996**, *749*, 257. (c) Mechref, Y.; Elrassi, Z. *Chirality* **1996**, *8*, 518. (d) Peterson, A.; Ahuja, E.; Foley, J. *J. Chromatogr., B* **1996**, *683*, 15. (e) Hara, S.; Dobashi, A. Japan Patent No. 92, **1992**, *149*, 205. (f) Hara, S.; Dobashi, A. Japan Patent No. 92, **1992**, *149*, 206. (g) Chu, D. Y.; Thomas, T. K. *Macromolecules* **1991**, *24*, 2212−2216. (h) Wang, J.; Warner, I. M. *Anal. Chem.* **1994**, *66*, 117−123. (i) Yrabe, H. H.; Shamsi, S. A.; Warner, I. M. *Anal. Chem.* **1999**, *71*, 3992−3999. (j) Palmer, C. P. *Electrophoresis* **2000**, *21*, 4054−4075. (k) Palmer, C. P.; Terabe, S. *J. Microcolumn Sep.* **1996**, *8*, 115−121. (l) Palmer, C. P.; Terabe, S. *Anal. Chem.* **1997**, *69*, 1852−1860. (m) Shamsi, S. A.; Akbey, C.; Warner, I. M. *Anal. Chem.* **1998**, *70*, 3078−3083. (n) Akbey, C.; Warner, I. M.; Shamsi, S. A. *Electrophoresis* **1999**, *20*, 145−151. (o) Hayenes, J. L., III; Billot, E. J.; Yarabe, H. H.; Warner, I. M.; Shamsi, S. A. *Electrophoresis* **2000**, *21*, 1597−1605.

(18) (a) Fuhrhop, J.; Helferich, W. *Chem. Rev.* **1993**, *93*, 1565. (b) Jaeger, D.; Kubicz-Loring, E.; Price, R.; Nakagawa, H. *Langmuir*, **1996**, *12*, 5803.

(19) (a) Zarif, L.; Polidori, A.; Pucci, B.; Gulik-Krzywicki, T.; Pavia, A.; Reiss, J. *Chem. Phys. Lipids* **1996**, *79*, 165. (b) Hato, M.; Minamikawa, H. *Langmuir* **1996**, *12*, 1658. (c) Seddon, J. *Ber. Bunsen-Ges. Phys. Chem.* **1996**, *100*, 380.

(20) (a) Miyagishi, S.; Nishida, M. *J. Colloid Interface Sci.* **1978**, *65*, 380. (b) Miyagishi, S.; Higashide, M.; Asakawa, T.; Nishida, M. *Langmuir* **1991**, *7*, 51. (c) Takehara, M.; Yoshimura, I.; Yoshida, R. *J. Am. Oil Chem. Soc.* **1974**, *51*, 419.

(21) (a) Tracey, A.; Radley, K. *Langmuir* **1990**, *6*, 1221. (b) Tracey, A.; Radley, K. *Mol. Cryst. Liq. Cryst.* **1985**, *122*, 77. (c) Tracey, A.; Radley, K. *J. Phys. Chem.* **1984**, *88*, 6044. (d) Radley, K.; Tracey, A. S. *Can. J. Chem.* **1985**, *63*, 95.

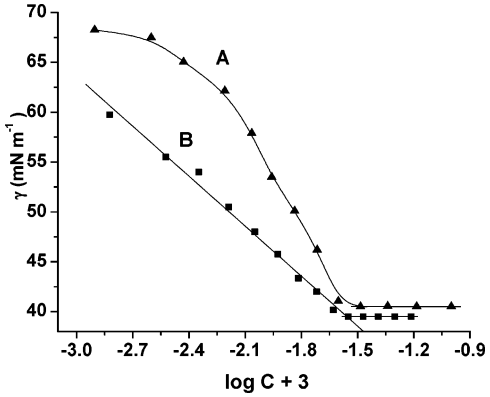

Figure 2. Plot of surface tension (γ) vs log C of SDLV in water (A) and 0.01 M NaOH (B).

facilitates aggregation. This is indicated by the nonlinear decrease of γ in the low concentration range.

In alkaline solution, the acid is completely dissociated and thus increases the electrostatic repulsion between headgroups, thus increasing the cac value as well as the surface area per surfactant headgroup. The surface area per surfactant molecule at the interface can be calculated from the slope of the linear part of the plot of γ versus log C using the Gibbs adsorption equation:[22]

$$\Gamma_m = -1/nRT\,(d\gamma/d \ln C) \quad (1)$$

$$A_m = 10^{18}/(\Gamma_m N_A) \quad (2)$$

where Γ_m is the maximum surface excess concentration expressed in mol m^{-2}, A_m is the minimum surface area (in nm^2) per surfactant molecule at the air/water interface, γ is the surface tension in mN m^{-1}, C is the concentration of surfactant, N_A is the Avogadro number, $R = 8.314$ J mol^{-1} K^{-1}, and $n = 2$ (for monovalent ionic surfactant). The value of A_m (0.57 nm^2) thus obtained is very small and indicates the generation of bilayer structures in dilute aqueous solution.[23] Similar values of A_m for other surfactants which form bilayer phases, for example, egg phosphatidylcholine ($A_m = 0.72$ nm^2)[1b] and *n*-alkylbetains ($A_m = 0.6$ nm^2),[1b] have been reported. However, the A_m value (1.1 nm^2) in NaOH solution of SDLV is almost twice that in water. This implies that the curvature of the aggregates in water is less than that in NaOH solution. Consequently, bilayer aggregates are expected to form in pure water.

Absorbance Spectra of SDLV. The UV−visible absorption spectra (see the Supporting Information) of a 0.125 mM solution of SDLV were measured in water (pH 7.5), in 0.01 M NaOH, and in a 50% (v/v) methanol−water mixture. The spectra have two absorption peaks centered at around 255 and 200 nm which correspond to $\pi \rightarrow \pi^*$ transitions originating from the benzene ring. The interesting feature of the spectrum is that in aqueous solutions, the long-wavelength absorption band tailed up to 600 nm, which is absent in the case of methanol solution. This can be attributed to the light-scattering properties of large molecular aggregates in aqueous solution. A bluish color of the solution, which is a signature of the presence of vesicles, was also observed. Upon standing overnight, gel-like fibrous aggregates were observed to appear in water at higher surfactant concentrations. In phosphate buffers (pH > 7.0) and NaOH solutions, no gel-like self-assemblies appeared upon aging. However, at pH = 6.0, the initially transparent solution upon overnight aging showed the formation of swarms or bundles of fibrous assemblies causing viscoelastic effects. The transition from transparent to gel-like phase becomes faster as the solution pH and concentration of the amphiphile were respectively decreased and increased. Indeed, aqueous solutions of SDLV at pH ≤ 5.0 transform into gel within a couple of hours. Therefore, it can be concluded that the appearance of gel-like assemblies in pure aqueous solution is a result of a slow decrease in pH due to absorption of atmospheric carbon dioxide, which shifts the equilibrium between carboxyl and carboxylate species toward the left. As discussed in the preceding section, the presence of carboxyl species in the self-assemblies reduces the ionic repulsion among headgroups and thus facilitates the formation of large aggregates. The shape and size of these fibrous aggregates have been discussed below.

Fluorescence Probe Studies. Fluorescence spectroscopy has been proved to be a useful technique to study the micropolarity of molecular self-assemblies of surfactant systems employing pyrene as a probe.[24−27] The intensities of the vibronic bands of the pyrene fluorescence spectrum strongly depend on the polarity of the environment. The intensity ratio of the first (I_1) to the third (I_3) vibronic bands of the pyrene fluorescence spectrum is commonly used as an indicator of the apparent micropolarity.[24,25] Thus the value of the I_1/I_3 ratio in 0.125 mM SDLV solution was observed to be 0.92, which corresponds to the dielectric constant of chlorobenzene ($\epsilon = 5.62$).[27] That is, the microenvironment of the probe in the self-assemblies has a polarity closely similar to that of a nonpolar solvent, suggesting solubilization of the fluorophore in the hydrophobic microdomain of the aggregate. The nonpolar microdomain of the aggregate is also indicated by the large blue shift of the fluorescence spectrum as well as by the large enhancement of the fluorescence intensity of *N*-phenyl-1-naphthylamine, NPN (inset of Figure 3), in the presence of SDLV above the cac in comparison to that in water.

To further investigate the microenvironment of the self-assemblies, we have measured the fluorescence intensity of 1,6-diphenylhexatriene (DPH) at various concentrations of the amphiphile. The plot of relative fluorescence intensity, I/I_0 (where I and I_0 are the intensities in the presence and absence of surfactant, respectively), as a function of surfactant concentration is shown in Figure 3. The inflection point of the plot gives the cac value (0.027 mM), which is very close to the value obtained from surface tension measurements. It can be seen that the fluorescence intensity of DPH increases by almost 15 times in the presence of 0.15 mM SDLV. As reported in the literature, the fluorescence quantum yield of DPH increases with solvent viscosity.[28] Therefore, the large increase of the fluorescence intensity of DPH at an amphiphile concentration greater than the cac indicates that its microenvironment is highly viscous. To substantiate this, we have also measured the steady-state fluorescence anisotropy (r) of DPH in the presence of SDLV at various temper-

(22) Ptak, M.; Egret-Charlier, M.; Sanson, A.; Bouloussa, O. *Biochim. Biophys. Acta* **1980**, *600*, 387−397.
(23) Won, Y.-Y.; Brannan, A. K.; Davis, H. T.; Bates, F. S. *J. Phys. Chem. B* **2002**, *106*, 3354−3364.
(24) Kalyansundaram, K. *Photophysics of Microheterogeneous Systems*; Academic Press: New York, 1988.
(25) Thomas, J. K. *The Chemistry of Excitation at Interfaces*; ACS Monograph 181; American Chemical Society: Washington, DC, 1984.
(26) Winnik, F. M.; Regismond, S. T. A. *Colloids Surf., A* **1996**, *118*, 1.
(27) Kalyanasundaram, K.; Thomas, J. K. *J. Am. Chem. Soc.* **1977**, *99*, 2039−2044.
(28) Cehelnik, E. D.; Cundall, J. R.; Lockwood, J. R.; Palmer, T. F. *J. Phys. Chem.* **1975**, *79*, 1369−1376.

Table 1. Surface and Self-Organization Properties of SDLV in Aqueous Solutions

sample	cmc/mM	γ_{cmc}/mN m^{-1}	A_m/nm^2	$N_{agg} \times 10^{-4}$	I_3/I_1 (ϵ)	anisotropy (r)	$D \times 10^{12}$/m^2 s^{-1}	R_H/nm
water	0.024	40.0	0.56	12	0.92	0.230	2.37	104.0
(pH 7.5)	(0.027)[a]				(5.62)			
0.01 M NaOH	0.028	39.5	1.1	3.6			4.58	56.0

[a] The data are obtained from fluorescence probe studies.

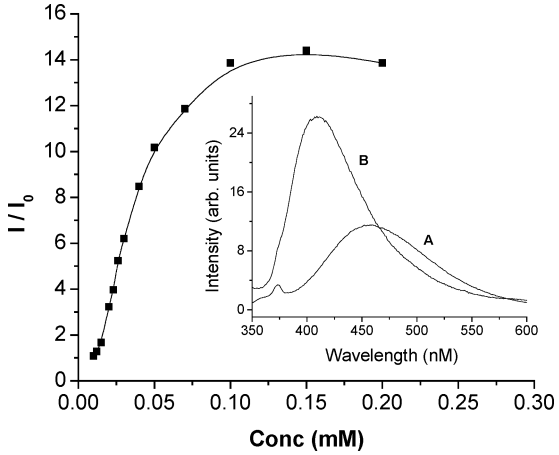

Figure 3. Plot of the relative fluorescence intensity (I/I_0) of DPH as a function of SDLV concentration. Inset: Fluorescence spectra of NPN in water in the absence (A) and in the presence (B) of 0.125 mM SDLV.

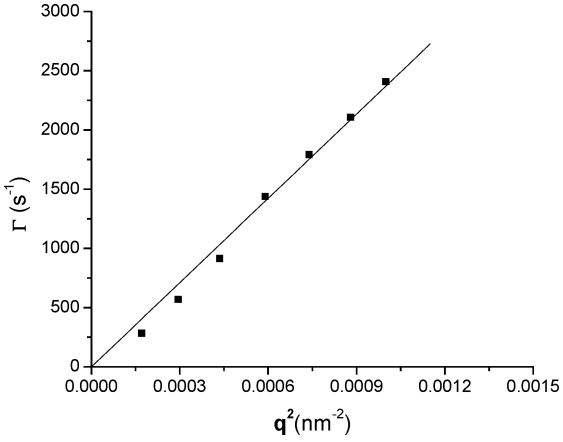

Figure 4. Plot of relaxation time, Γ, of the self-assemblies in a 0.125 mM solution of SDLV as a function of the square of the scattering vector, q^2.

atures. For a 1 mM SDLV solution, the anisotropy value initially increases with temperature and then starts to fall off at higher temperatures (see the Supporting Information). The maximum value (∼0.230) of r was obtained at 30 °C. A similar value of fluorescence anisotropy has been reported for liposomes.[29]

The high anisotropy value of the probe at room temperature suggests that the probe is solubilized in a rigid environment. The increased rigidity (i.e., viscosity) of the microenvironment is a result of tight packing of the hydrocarbon chains of the amphiphile. This means that the aggregates formed by SDLV have bilayer type structures. The ordering of the interface of the aggregates reduces the degree of water penetration in the hydrocarbon layer, in accordance with the reduction observed in micropolarity sensed by the probe molecules. The low anisotropy values at low and high temperatures may be due to either a decrease in packing of the surfactant tails or the transformation of bilayer structures to smaller aggregates such as micelles.

Light Scattering Studies. DLS measurements were performed to obtain the mean size and size distribution of the self-assemblies in dilute solutions. A cumulant analysis of the intensity autocorrelation function,[30,31] $g^{(2)}(\tau)$, resulted in an apparent diffusion coefficient $D = \Gamma/q^2$, where Γ and q are respectively the decay rate and scattering vector. The scattering vector $q = (4\pi n/\lambda_0) \sin(\theta/2)$, where n is the refractive index of the dispersing medium, λ_0 is the vacuum wavelength of the incident light, and θ is the scattering angle. A plot of the relaxation rates versus q^2 values is shown in Figure 4.

The plot is linear and passes through the origin, suggesting that the apparent diffusion coefficient is due to Brownian motion of the particles. The dependence of the relaxation rate on the scattering angle also implies angular dependence of the diffusion constant and hence of the hydrodynamic radius. This means that the self-assemblies are polydisperse. Indeed, a relatively high polydispersity index (∼1.3) was recorded in DLS measurement with a 0.125 mM SDLV solution. The slope of the straight line (2.37×10^{-12} m^2 s^{-1}) gives the average diffusion coefficient of the aggregates. The apparent diffusion coefficient of the amphiphile is $\sim 10^{-12}$ m^2 s^{-1} (see Table 1), which is much smaller than that of normal spherical micelles[32] for which the diffusion constant is of the order of 10^{-10} m^2 s^{-1}. For such a system, assuming spherical shape of the particles, the apparent diffusion coefficient, D, can be related to the hydrodynamic radius, R_H, through the Debye−Stokes−Einstein relationship:

$$R_H = k_B T/6\pi\eta D \qquad (3)$$

where k_B is the Boltzmann constant, T is the absolute temperature, and η is the viscosity of the dispersing medium. The R_H value (104 nm) calculated from the above equation is listed in Table 1. In the case of NaOH solution, the R_H value (56 nm) is almost half the value in water. However, these values are far too large to represent a spherical micelle. Therefore, these aggregates can be either multilamellar spherical vesicles or tubules and ribbons. The DLS measurements were done within 1 h of sample preparation. These results are consistent with those obtained from surface tension and absorbance measurements. The mean aggregation number of the large aggregates can be obtained from the measured A_m and R_H values using the equation[33]

$$N_{agg} = 4\pi(R_H)^2/A_m \qquad (4)$$

The N_{agg} values thus obtained are listed in Table 1. The N_{agg} values are very high. Similar large values of N_{agg}

(29) (a) Cogan, U.; Schinitzky, M.; Weber, G.; Nishida, T. *Biochemistry* **1973**, *12*, 521. (b) Zachariasse, K. A.; Kuhnle, W.; Weller, A. *Chem. Phys. Lett.* **1980**, *73*, 6.
(30) Koppel, D. E. *J. Chem. Phys.* **1972**, *57*, 4817.
(31) Berne, B. J.; Pecora, R. *Dynamic Light Scattering*; Wiley-Interscience: New York, 1976.
(32) Hassan, P. A.; Raghavan, S. R.; Kaler, E. W. *Langmuir* **2002**, *18*, 2543−2548.
(33) Christov, N. C.; Denkov, N. D.; Kralchevsky, P. A.; Broze, G.; Mehreteab, A. *Langmuir* **2002**, *18*, 7880−7886.

Table 2. Absorption Frequencies of FT-IR Spectra of SDLV

solvent	N−H stretching (cm^{-1})	amide-I (C═O stretching) (cm^{-1})	amide-II (N−H bending) (cm^{-1})
KBr	3365	1630	1610
water (1 mM)	3385	1652	1608
THF (1 mM)	3365	1664	1608

have also been reported for other amphiphiles forming bilayer structures.[33] The high value of N_{agg} is consistent with the large value of R_H of the aggregates. The results of DLS studies thus rule out the existence of small micelles and confirm the presence of large bilayer aggregates even in a dilute aqueous solution of SDLV.

FT-IR Spectra. To explain the nature of molecular interactions responsible for the formation of large aggregates, we have measured the FT-IR spectra (not shown here) of SDLV in a KBr pellet and for dilute solutions (1 mM) in water and tetrahydrofuran (THF) solvents. The corresponding absorption frequencies of the amide bond are listed in Table 2. The spectra showed almost identical absorption bands. The band at 3385 cm^{-1} indicates the presence of hydrogen-bonded −NH− groups. That the amide group is hydrogen-bonded is further confirmed by the frequencies of the amide-I and amide-II bands at 1652 and 1608 cm^{-1}, respectively. The intermolecular amide hydrogen bonding has also been reported by other authors for many NAASs.[14,15]

The molecular structure (see Figure 1) of SDLV shows that there can be a stable intermolecular hydrogen bond between −NH− and −CO− in the amide group that induces a stable linear state. The influence of the amide linkage at the hydrophilic headgroup on the aggregation properties of NAASs has already been established in the literature.[34]

Our FT-IR results also indicate intermolecular hydrogen bonding between the amide groups of neighboring SDLV molecules in the self-assemblies. This amide−amide intermolecular hydrogen bonding results in a flat-layered structure. The low values of cac and A_m of SDLV compared to those of the corresponding fatty acid salt indicate that the intermolecular hydrogen-bonding interaction between amide groups and the π stacking interaction between benzene rings enhance the hydrophobic interaction between chains. This is further strengthened by the homochiral interaction between amino acid headgroups. Although the tendency of NAASs to associate by hydrogen-bonding interactions is reduced by the formation of equally strong amide−water hydrogen bonds, the secondary amide hydrogen-bond chains have been found to be very useful as a stabilizing factor to overcome hydration energies. This means that the solvation of the hydrophilic amide group near the chiral carbon is lost during aggregation and the self-assembly is favored by the intermolecular hydrogen bonding. Indeed, the two-layer arrays of the intermolecular hydrogen-bonding interactions through the amide bonds of the neighboring surfactant molecules result in the formation of a parallel arrangement of the corresponding hydrophobic tails such that the SDLV molecules can self-organize into bilayer structures in water. The ordered bilayer membranes are formed not only from enantiomeric molecules but also from achiral molecules. For example, in a recent report, we have shown the existence of tubular and lamellar bilayer vesicles in dilute aqueous solutions of sodium 11-acrylamidoundecanoate.[9a]

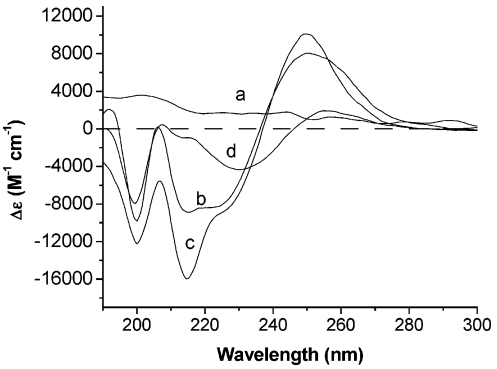

Figure 5. Circular dichroism spectra of SDLV in water: (a) 0.015 mM, (b) 0.125 mM, (c) 0.5 mM, and (d) in methanol (0.5 mM).

The bilayer sheets with strong surface binding interactions tend to form helical ribbons and mono- or multilayer tubules. The existence of bilayer vesicles is also manifested by the high fluorescence anisotropy value (i.e., low fluidity) and low polarity of the microdomains of the self-assemblies. Low microfluidity has also been reported for phospholipid vesicles.[29] These assemblies were formed from lamellae of a bilayer of molecules in which the amphiphiles were oriented either head to head or tail to tail. The intermolecular hydrogen bonding between the amide groups aligns the amphiphile molecules to form such lamellae and stabilizes the aggregates.

Circular Dichroism Spectra. The lamellar structure of SDLV as discussed above can get twisted due to the presence of the chiral center, and therefore helical ribbons and rodlike aggregates are also expected to be present in solution. In fact, the homochiral interactions between the chiral groups have been proposed to account for the twisting to form the helices.[35] If the chiral superstructures are formed along with the bilayer structures, then one can expect the existence of a characteristic CD band and its concentration dependence in water. Therefore, the aqueous solution of SDLV was also analyzed for chiral organization by CD spectroscopy. The CD spectra (Figure 5) were recorded in aqueous solutions of concentrations above and below the cac value and in methanol solution, where the surfactant molecules are not aggregated. At concentrations above the cac, the CD spectra of SDLV in water exhibit three bands at 200, 215, and 250 nm. A band at 225 nm also appears as a shoulder to the 215 nm band.

Since there is no absorption due to SDLV in the wavelength region of 200−240 nm, the new CD bands belong to the solution system and indicate formation of chiral aggregates of SDLV in water. The intensity of the bands decreases as the concentration of SDLV decreases, and finally the bands disappear at concentrations below the cac value. As can be seen in Figure 5, the spectrum of 0.015 mM SDLV only shows a weak and broad positive band in the range of 300−200 nm. Thus there is a marked change in the CD spectrum that accompanies micelle formation. The disappearance of the CD band systems at a concentration below the cac suggests that the chiral structure is formed through aggregation. To further confirm this, we have measured the CD spectrum in pure methanol solvent containing 0.5 mM SDLV. The spectrum exhibits three band systems at 200, 230, and 255 nm. The band at 215 nm completely disappeared, and the shoulder at 225 nm developed into a peak in methanol. However, the intensity of the bands is much weaker compared to

(34) Yeoh, K. W.; Chew, C. H.; Gan, L. M.; Koh, L. L.; Teo, H. H. *J. Macromol. Sci., Chem. A* **1989**, *26*, 663−680.

(35) Helfrich, W.; Prost, J. *Phys. Rev. A* **1988**, *38*, 3065.

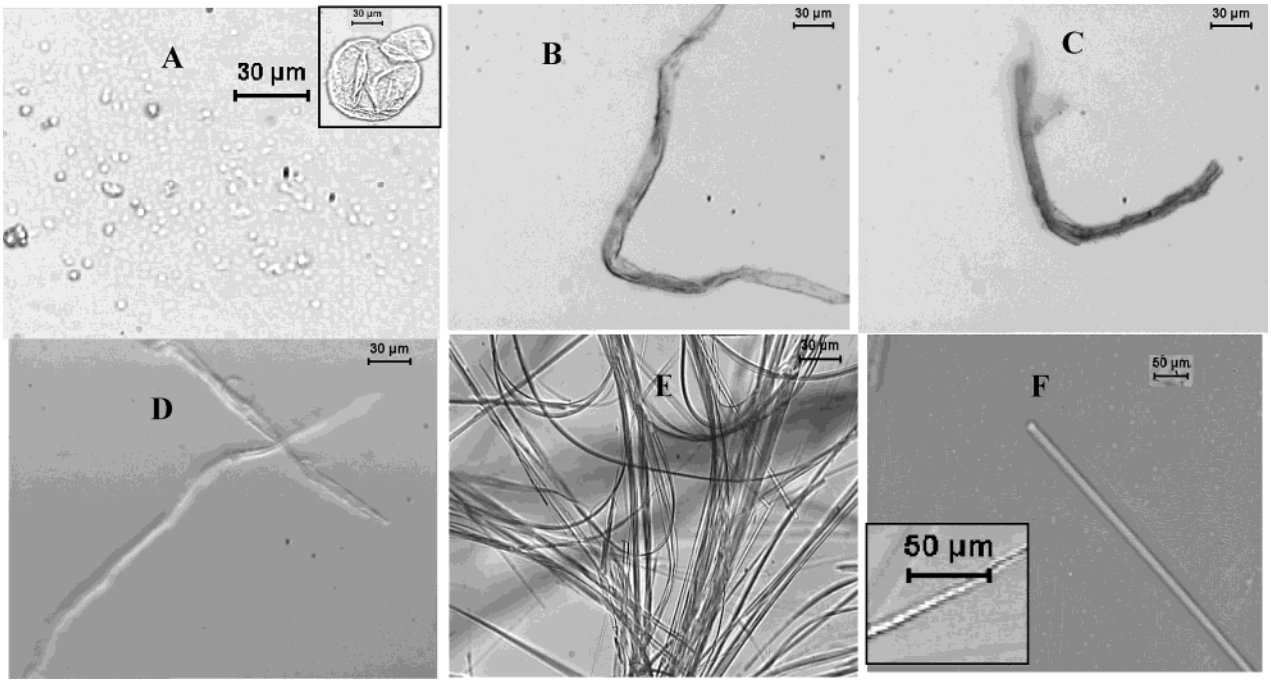

Figure 6. Optical micrographs of a 1 mM solution of SDLV: (A) vesicles, (B) twisted ribbon, (C) two-strand helix, (D) twisted ribbon and tubules, (E) 3D network structure of entangled fibers, and (F) tubules (inset: two-strand helices).

those of the corresponding spectrum in aqueous solution. Similar CD spectral features have also been observed for other NAASs in methanol and have been attributed to chiral liquid crystalline structures.[36]

The existence of chiral superstructures is manifested by the CD spectra of SDLV in aqueous solution. The 250 nm band in the CD spectra corresponds to the $\pi \rightarrow \pi^*$ electronic transitions originating from the benzene chromophore. The CD peak at 212 nm could be associated with the $\pi \rightarrow \pi^*$ transition of the amide bond, and the shoulder at ~222 nm is thought to have originated from the $n \rightarrow \pi^*$ transition.[37−39] The CD band at 200 nm, which appears at all concentrations, can be attributed to the asymmetric structure of the optically active SDLV molecule. The CD spectra of the chiral micelles of SDLV appear to be different from those reported for amide organization in α-helix, β-sheet, or random assembly of proteins. The CD spectra have similarity with those of *N*-palmitoyl- or *N*-stearoyl-L-serine amphiphile in water.[15a] This unique spectral feature as suggested by Shinitzky et al. is due to a network of the amide bonds with a distinct chiral feature.[15a] The results described above indicate that the CD spectra of SDLV are due to amide organization in α-helix form. Similar helical structures of chiral aggregates have also been reported for *N*-acylamino acid surfactants by other authors.[13−15]

Microscopic Studies. To investigate the microstructure of the self-assemblies of SDLV, both optical and transmission electron micrographs were measured in aqueous solution. The optical micrographs (Figure 6A−F) of a 1 mM solution of SDLV in water revealed various morphologies. Micrographs A−D were obtained from the same solution after 2 h of sample preparation. Both spherical and elongated vesicles can be observed in picture A. The outer diameter of the vesicles is in the range of 4−6 μm, and the wall thickness, of 0.8 μm. The value of the wall thickness suggests multilayer vesicles. The inner diameter of the vesicles is in the range of 2−4 μm. Micrograph B exhibits a twisted ribbon structure, the width of which is ~15 μm. The length of the ribbons is in the millimeter range. Figure 6C shows the presence of a two-strand helical structure. The existence of tubules can be observed in picture D. The tubules are long with a width of ~15 μm. The channel of the tubes is about 8 μm. Micrograph D also shows twisted ribbon structures. Tubular microstructures of this type have also been reported for similar NAASs.[13f,14b]

The optical micrographs (Figure 6E,F) of SDLV in phosphate buffer at pH 6.0 that showed viscoelastic effects exhibit three-dimensional network structures consisting of long, entangled flexible fibers. This explains the appearance of gel-like aggregates in solutions of pH < 7.0. Double helical ropes are also found in the solution (see the inset of picture F). The fibers are in fact long tubules as can be seen in picture F. The tube diameter (o.d.) is in the range of 2−3 μm. The wall thickness is about 500 nm, which means that the fibers are multilayered tubules.

The samples (1 mM SDLV) for transmission electron micrographs were made in water immediately before measurement. The TEM images are depicted in Figure 7A−F. The electron micrographs, in consistence with the optical micrographs, also exhibit a variety of morphologies including networks of multilayer spherical vesicles (Figure 7A−C), bilayer tubules (Figure 7C), rodlike structures (7D), long helical ribbons (7E), and long helical strands (7F). Both mono- and multilayer vesicles of different sizes can be observed. The wall thickness of the spherical vesicles is in the range of 40−200 nm. The vesicles corresponding to a layer thickness of 40 nm are monolayer vesicles, and the ones with a layer thickness greater than 40 nm are multilayer vesicles. The tubules have an outer diameter in the range of 20 μm and have a length in the millimeter range. The tubules are hollow and filled with fluid. Because of the low contrast of the images, it was

(36) (a) Sakamoto, K.; Yoshida, R.; Hatano, M. *Chem. Lett.* **1976**, 1401. (b) Sakamoto, K.; Yoshida, R.; Hatano, M.; Tachibana, T. *J. Am. Chem. Soc.* **1978**, *100*, 6898.
(37) Moffitt, W. *J. Chem. Phys.* **1956**, *25*, 467.
(38) Gratzer, W. B.; Holtzwarth, G. M.; Doty, P. *Proc. Natl. Acad. Sci. U.S.A.* **1961**, *47*, 1785.
(39) Rosenheck, K.; Sommer, B. *J. Chem. Phys.* **1967**, *46*, 532.

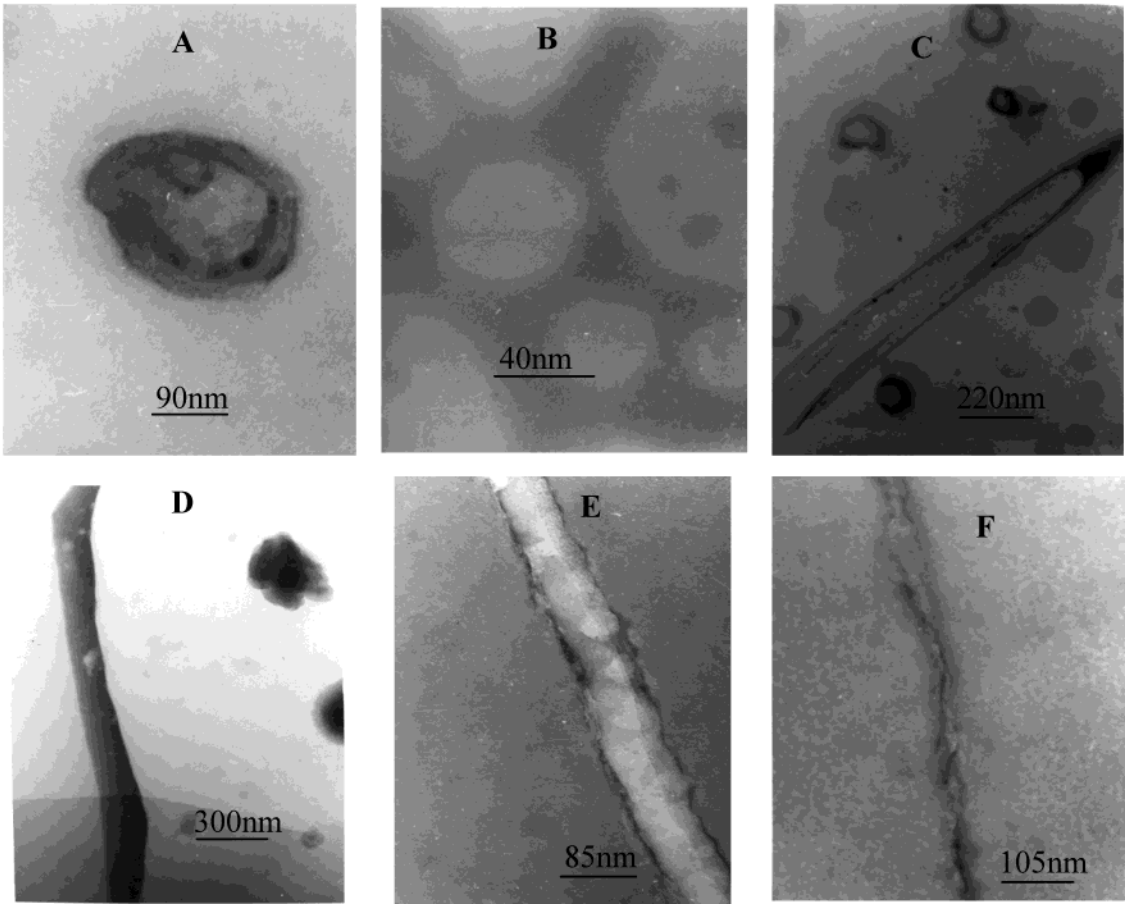

Figure 7. Negatively stained transmission electron micrographs of a 1 mM solution of SDLV: (A) multilayer vesicles, (B) network of vesicles, (C) tubules and vesicles, (D) micellar rod, (E), helical ribbon, and (F) two-strand helix.

difficult to measure the pitch level of the twisted ribbons and helical strands in the micrographs. The helical ribbon in picture 7B has transformed almost to a tubule, indicating that the tubes might have formed from ribbons. It seems that the structure in picture 7F represents a two-strand helix. The fact that these micrographs were obtained from the same samples suggests that all the structures that coexist were spontaneously formed in solution. These structures were obtained in the concentration range of 0.125−4 mM. However, the size of the self-assemblies seen in the TEM images does not reflect the diameter of the vesicles in aqueous solution because the vesicles are broken randomly during sample preparation.

Conclusions

Sodium *N*-(4-dodecyloxybenzoyl)-L-valinate, which has low cac and γ_{cmc} values, is a very good surface active agent. Surface tension and fluorescence studies have indicated the formation of bilayer structures of SDLV in water. The molecular self-assemblies have a very low translational diffusion coefficient and thus have a large apparent hydrodynamic radius. The average aggregation number of the amphiphile is also very high. These data suggest that the amphiphile forms large bilayer aggregates in dilute aqueous solution. The fluorescence probe studies indicate that the microenvironment of the self-assemblies is nonpolar and is very viscous, indicating a rigid core. The CD spectra and the microscopic images of dilute solutions of SDLV have also indicated formation of chiral aggregates like twisted (or helical) ribbons and helical strands. In fact, depending upon the concentration a variety of morphologies of the organized self-assemblies, for example, spherical vesicles, tubules, ribbons, double helical ropes, and rods, were observed. The spherical vesicles are abundant in dilute solutions, whereas other bilayer structures are predominantly present in relatively concentrated solutions. The existence of tubular structures suggests that ordered bilayer membranes are spontaneously formed from the amphiphile in aqueous solution. We believe that the flat lamellae scroll up like cigarette paper to form tubules and rodlike aggregates. The driving forces for the bilayer formation are (i) hydrophobic interaction among hydrocarbon chains, (ii) $\pi-\pi$ interaction between aromatic rings, and (iii) intermolecular hydrogen bonding between the secondary amide groups of the neighboring molecules, which promote the formation of linear arrays of the amphiphile molecules.

Experimental Section

Materials. The fluorescence probe pyrene, NPN, and DPH (Aldrich) were purified by repeated recrystallization from acetone−ethanol mixtures. The purity of the compounds was confirmed by measuring fluorescence emission and excitation spectra at various wavelengths. Analytical grade sodium hydroxide (SRL), potassium carbonate, sodium chloride, and phosphotungstic acid (SRL) were procured locally and were used directly from the bottle. All solvents used were good-quality commercial products and whenever necessary were purified, dried, and distilled fresh before use.

The synthesis of *N*-(4-dodecyloxybenzoyl)-L-valine (DDLV) has already been reported elsewhere.[8] Briefly, 4-dodecyloxybenzoic acid was first synthesized from 4-hydroxybenzoic acid and 1-bromododecane and purified according to the reported procedure.[40] The coupling of L-valine and 4-dodecyloxybenzoic acid

was made via the formation of NHS ester in the presence of DCC.[41] The acid was recrystallized two or three times from an ethanol−water mixture to eliminate DCU, a byproduct of the reaction. The sodium salt was prepared by stirring equimolar mixtures of sodium methoxide and *N*-(4-dodecyloxybenzoyl)-L-valine in dry methanol for 6−8 h. The salt was obtained after evaporation of the solvent. It was recrystallized from ethanol−water until it was free from unreacted acid. The structure was confirmed by IR and ^{1}H NMR spectra.

General Instrumentation. ^{1}H NMR spectra were recorded on a Bruker SEM 200 instrument in $CDCl_3$ solvent using TMS as the standard. The FT-IR spectra in aqueous solution and in a KBr pellet were measured with a Thermo Nicolet Nexus 870 spectrometer. A thin layer of a 1.0 mM solution of the compound was placed between zinc selenide plates. The background spectrum of the pure solvent was subtracted from the raw data using the instrumental software.

The UV−visible spectra were recorded on a Shimadzu model 1600 spectrophotometer. The circular dichroism spectra were measured with a Jasco J-810 spectropolarimeter using a quartz cell with a path length of 2 or 10 mm. The measurement of specific rotation was performed with a Jasco P-1020 digital polarimeter. The steady-state fluorescence spectra were measured on a SPEX Fluorolog model FL3-11 spectrofluorometer. The surface tension measurements were performed using a Torsion Balance (S.D. Hurdson & Co., Calcutta) using the Du Nuoy ring method. Melting points were determined with an Instind (Calcutta) melting point apparatus in open capillaries. The pH measurements were done with a digital pH meter model pH 5652 (EC India Ltd., Calcutta) using a glass electrode.

Surface Tension Measurement. A stock solution of SDLV was made in Milli-Q water (18.2 MΩ). An aliquot of this solution was transferred to a beaker containing a known volume of water. The solution was gently stirred magnetically and allowed to stand for about 5 min at room temperature (~28 °C), and then the surface tension was measured. For each measurement, at least three readings were taken and the mean γ (mN m^{-1}) value was recorded. Before each experiment, the instrument was calibrated and checked by measuring the surface tension of distilled water. The critical micelle concentration (cmc) value was obtained from the break point of the plot of γ versus log C.

Fluorescence Measurements. The steady-state fluorescence spectra of pyrene, NPN, and DPH probes were measured in the presence of various concentrations of the amphiphile in the range of 5×10^{-6} to 1×10^{-3} M. A saturated solution of the probe was divided into two parts. One part of this was used to prepare a stock solution (1 mM) of SDLV, and the other part was used for dilutions required to make solutions of varying concentration. The pyrene solutions were excited at 335 nm, and the spectra were recorded in the wavelength range of 350−500 nm. On the other hand, the DPH solutions were excited at 350 nm and the spectra were recorded in the wavelength range of 370−550 nm. Each spectrum was blank subtracted and corrected for monochromator efficiency. To eliminate the effect of time-dependent lamp intensity change, the spectra were recorded with the S/R setting. The steady-state fluorescence spectra were measured at ~25 °C.

Steady-state fluorescence anisotropies of DPH in the presence of SDLV were measured in a Perkin-Elmer LS-55 luminescence spectrometer equipped with polarizers upon excitation at 350 nm. The fluorescence intensity was measured at 430 nm. The excitation and emission slit widths were 2.5 and 10 nm, respectively. The fluorescence anisotropy values (r) at each temperature were calculated by use of the equation

$$r = (I_{VV} - GI_{VH})/(I_{VV} + 2GI_{VH}) \quad (5)$$

where I_{VV} and I_{VH} are respectively the fluorescence intensities of the emitted light polarized parallel and perpendicular to the excited light, and G ($=I_{VV}/I_{VH}$) is the instrumental grating factor.

Light Scattering Measurement. The DLS measurements were performed using a Photal DLS-7000 (Otsuka Electronics Co. Ltd., Osaka, Japan) optical system equipped with an Ar^+ ion laser (75 mW) operated at an output power of 16 mW at $\lambda_0 = 488$ nm, a digital correlator, and a computer-controlled and stepping-motor-driven variable angle detection system. The solution of the amphiphile was prepared in Milli-Q water and was filtered directly into the quartz cell by use of a Millex-GV (Millipore) membrane filter (0.22 μm). The quartz cell was rinsed several times with filtered water and then filled with the filtered sample solution. The DLS measurements began 5−10 min after the sample cell was placed in the DLS optical system. For all light scattering measurements, the temperature was 25 ± 0.5 °C.

Optical and Transmission Electron Microscopy. For both optical and transmission electron microscopic measurements, the surfactant solution was filtered by use of a one-way syringe membrane filter (0.22 μm). A drop of the aqueous surfactant solution (1 mM) was placed on the carbon-coated copper grids, blotted with filter paper, and negatively stained with a freshly prepared 2% aqueous solution of phosphotungstic acid. The specimens were examined on a Phillips CM 12 electron microscope operating at 80 kV at room temperature (~25 °C).

For optical micrographs, the filtered solution was first degassed in an ultrasonic bath for 10 min. A drop of the appropriate solution was placed on a thoroughly cleaned glass plate. The light micrographs were obtained with a Leica-DMRXP microscope. The images taken by a video camera were analyzed by Leica Qwin software.

Acknowledgment. The work presented in this paper is supported by CSIR (Grant No. 01(1664)/00/EMR-II) and DST (Grant No. SP/S1/G-36/99), Government of India. The authors are thankful to Professor B. Mishra for measurements with the optical microscope.

Supporting Information Available: The details of turbidity studies including the absorbance spectra, the time dependence of absorbance, and the temperature dependence of fluorescence anisotropy study. This material is available free of charge via the Internet at http://pubs.acs.org.

LA035958X

(40) Bhattacharya, S.; Subramanian, M.; Hiremath, U. S. *Chem. Phys. Lipids* **1995**, *78*, 177−188.

(41) Lapidot, Y.; Rappoport, S.; Wolman, Y. *J. Lipid Res.* **1967**, *8*, 142−145.